Silver-halide valence and conduction states: Temperature-dependent ultraviolet-photoemission studies*

R. S. Bauer
Xerox Palo Alto Research Center, Palo Alto, California 94304

W. E. Spicer
Stanford Electronics Laboratories, Stanford University, Stanford, California 94305

(Received 15 April 1976)

The electronic states of AgBr, AgCl, and β-AgI were studied using photoemission spectroscopy at temperatures T between 80 and 295°K for photon energies $h\nu$ from threshold (7.15, 7.55, and 6.6 ± 0.1 eV, respectively) through 21.2 eV. Without using theoretical band-structure information, the atomic origin and in some cases Brillouin-zone location are determined by the $h\nu$ and T variations of energy-distribution-curve structure. We unambiguously identify the filled states of almost pure $4d_{5/2}$ symmetry at -3.7, -3.3, and -4.4 ± 0.1 eV below the valence-band maximum in AgBr, AgCl, and β-AgI, respectively. The halogen p-derived valence states are all highly hybridized with Ag $4d$ states and are characterized by two large density-of-states regions at -0.85 and 2.9; -0.8 and -2.65; -0.45 and -1.7 eV in AgBr, AgCl, and β-AgI, respectively. The halogen peak closest to the valence-band maximum probably has a symmetry other than Γ. A secondary peak of mainly d character is identified in the density of AgBr valence states at -1.95 eV. Using Mason's x-ray photoemission results, we locate similar structure at -1.6 eV in AgCl and -1.1 eV in β-AgI. In addition, the lower Ag ($4d_{3/2}$) derived hybridized states are located at -5.0 eV in AgBr and result in a 6.0-eV valence-band width. The photoemission clearly shows the Γ nature of the β-AgI valence-band maximum; the band gap is direct only in β-AgI, as expected from its wurtzite rather than rock-salt crystal structure. We report the first measurement of silver-halide conduction-state features. Large density-of-states regions are found at 7.3, 8.1, and 7.1, and 7.8 eV above the valence-band maximum in AgBr, AgCl, and β-AgI, respectively; these are probably derived from the halogen d states. The Ag $5p$ conduction states have a large density at 8.8 and 9.3 eV in AgBr and 9.85 eV in AgCl. Strong atomic and k-conservation selection rules dominate the optical excitation process. These are used to identify other conduction-state features; for example, in β-AgI the I($5d$) $\Gamma_{25'}$ state occurs at 8.0 ± 0.2 eV and the Ag($5p$) $\Gamma_{2'}$ level is at 10.1 ± 0.2 eV. Comparison is made to other measurements and to band-structure calculations.

I. INTRODUCTION

In this paper we demonstrate that the temperature dependence of ultraviolet-photoemission energy-distribution curves (EDC's) can be used to separate hybridized states from neighboring levels having mainly the symmetry of a single atomic orbital. Generally speaking, the valence states of solids which have an ionicity midway between pure covalent and pure ionic ($0.86 > f_i > 0.73$) and certain conduction states of more ionic materials ($1 > f_i > 0.86$) should exhibit the necessary dynamic hybridization. Here we concentrate on the silver halides AgBr, AgCl, and β-AgI, emphasizing their common electronic-state characteristics.

The salient features of this novel technique are clear from Figs. 1 and 2 which show AgBr and AgCl data. Only certain EDC structures exhibit thermal broadening that is greater than $10k_B\Delta T$. This selectivity is understood as a lattice vibration modulation of the orbital hybridization; a simple-model calculation[1] of this process for AgBr predicts the correct order of magnitude for both the broadening of the hybridized state density and its temperature dependence. It follows that neighboring pure symmetry states will only broaden by the normal change in thermal energy $k_B\Delta T$. This must then be the nature of the states at -3.7 eV in AgBr [Fig. 2(a)] and at -3.3 eV in AgCl [Fig. 2(b)]. One can further confidently assign them to Ag $4d_{5/2}$ orbitals since such states must lie below the valence band maximum and by symmetry cannot all hybridize with neighboring halogen p orbitals.

Other photoelectron spectroscopic investigations in different $h\nu$ ranges were performed on AgBr,[2-4] AgCl,[2-4] and β-AgI,[3-6] following our first ultraviolet-photoemission studies of these solids.[7] Assignments in all these cases were made on the basis of band-structure calculations with the addition of a photoionization cross-section model in Refs. 2 and 6. Further, they were all limited to identifications of valence levels only. In this paper we discuss the nature of the filled states from the $h\nu$ and T dependencies of the EDC's. Only then do we compare our results to band calculations and other experiments. We further are able to

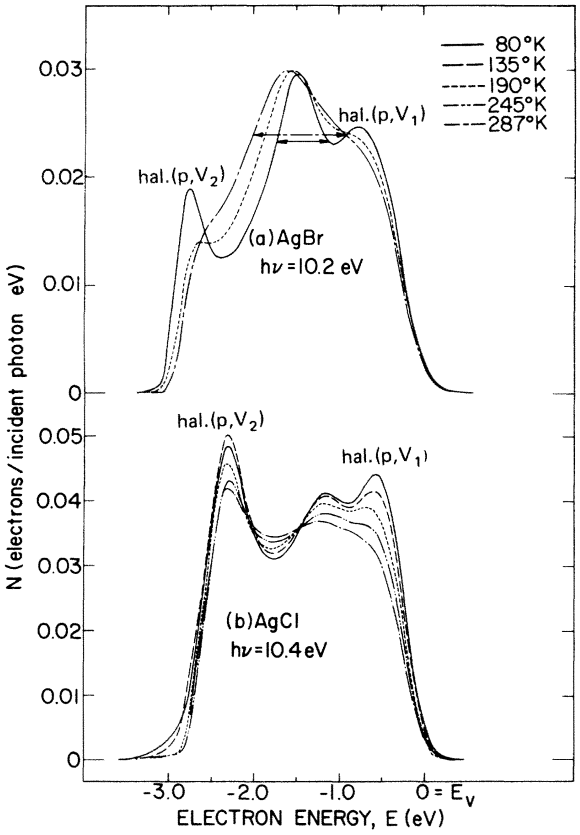

FIG. 1. Comparison of energy distributions normalized to quantum yield (per incident photon) for electrons photoemitted from (a) AgBr and (b) AgCl at 80–287 °K for photon energies of 10.2 and 10.4 eV, respectively. The arrows indicate the state density broadenings due to dynamic hybridization, as calculated in Ref. 1. EDC structure is labeled according to its atomic and band origins [e.g., halogen p valence—hal.(p, V)].

extend this process to the empty states, thereby directly measuring conduction band features for the first time. The unique EDC nature of k-conserving transitions is used to identify symmetry characteristics of some of the states.

II. EXPERIMENT

A. Sample preparation

The silver-halide samples used in these studies were crystalline thin films evaporated in the experimental chamber from 99.999% pure powder. Deposition rates were typically 1–3 Å/sec as measured by a quartz crystal microbalance. Chamber pressure rose to a maximum of 3×10^{-8} Torr during deposition from 4×10^{-11} Torr typical of measurement conditions. The 99.99% pure silver (and occasionally platinum) substrates were heat cleaned at 450° C and 1×10^{-10} Torr prior to deposition. Film thickness was limited to 200–400 Å in order to eliminate severe EDC distortions due to charging at low temperatures in thick (6000-Å) films. The photoemission from these very thin films was identical to that of the thick samples. Data were reproducible among samples, did not change after 20 cooling cycles, and showed no photolytic decomposition effects after a month of uv measurement. The substrate temperature during growth ($175 > T_s > 22$° C) or subsequent annealing (150° C $> T_A$) did not significantly effect EDC characteristics. Surface contamination caused by exposure to air was minimal, but cesium was found to react with the silver halides.

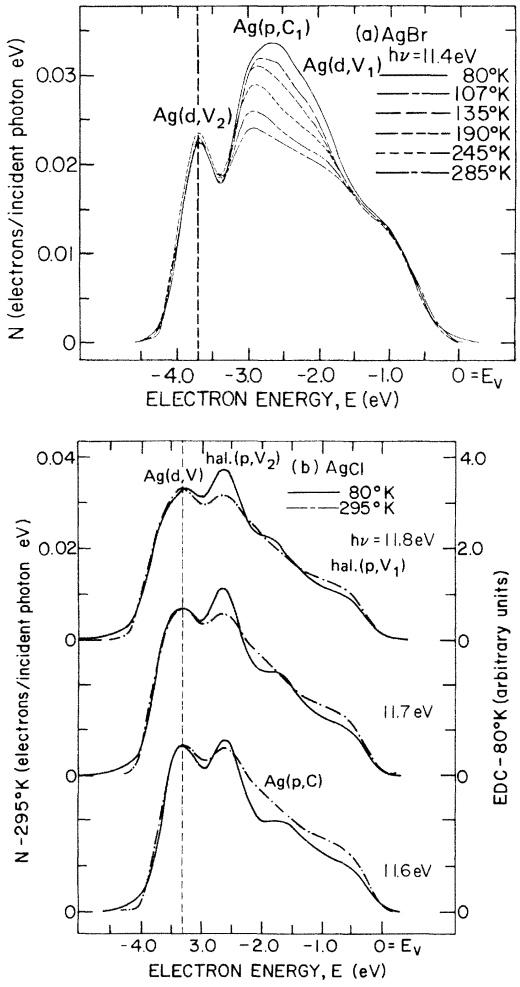

FIG. 2. Comparison of energy distributions for electrons photoemitted from (a) AgBr and (b) AgCl at 80–295 °K for the photon energies indicated. Lines are shown at electron energies of (a) −3.7 eV and (b) −3.3 eV. The 80 °K AgCl data in part (b) are unnormalized, with the −3.3-eV peak height adjusted to the value of the corresponding 295 °K peak. EDC structure is labeled according to its atomic and band origins [e.g., silver d valence—Ag(d, V) and silver p conduction—Ag(p, C)].

The photon energy range was extended beyond 11.8 eV by knocking off the LiF window from the chamber while it was attached to the McPhearson 225 monochromator. In this case the sample could not be cooled because of the relatively poor vacuum conditions. Room-temperature results agree with ultrahigh-vacuum measurements, though increased electron scattering is evident in the data. An extremely detailed discussion of sample characteristics is presented in Ref. 7.

B. Data

Sample temperature was set and maintained to ±4°K by flowing gas chilled with a liquid-nitrogen heat exchanger through the sample holder.[7,8] The silver-halide photoemitter was surrounded by a cylindrical collector; it had a 98% transmitting screen attached over the front hole to improve electric field geometry.[9] Standard electronic techniques were used for measuring EDC's.[10] The net photon and electron energy resolution was between 0.10 and 0.15 eV.

In order to determine the origin of EDC structure, it is very useful to summarize the experimental information in a plot of the final-state energy of each peak and shoulder as a function of photon energy. Such structure plots for the silver halides are presented in Fig. 3. As an example, note that the four AgCl structures and end points of the EDC's shown in Fig. 2(b) are summarized by six points in Fig. 3(b) for each of the photon energies. Though vital information on magnitude and width has been discarded, systematics in position alone allow high-density-of-state regions to be identified. Transitions from regions of high valence-state density produce EDC structure which changes position by the increment in photon energy, while transitions to conduction states have $h\nu$-independent final-state electron energies. Then the electron-energy-axis intercept of zero-slope structure is the energy of empty state peaks while unity-slope structure intercepts at the filled state energy. Using Fig. 3 we can immediately identify three valence-band peaks in each solid and one (AgCl) or two conduction-band features.

No assumptions about the optical excitation process are necessary to locate high-density-of-state regions in this way. If k conservation is not an important selection rule, then the structure corresponding to these density of states regions will behave in the manner described due to conservation of energy. If k is conserved, then this behavior can occur for transitions between the high-density-of-states region and a sharply changing band in the same region of the Brillouin zone.

The highest filled state is determined by extrap-

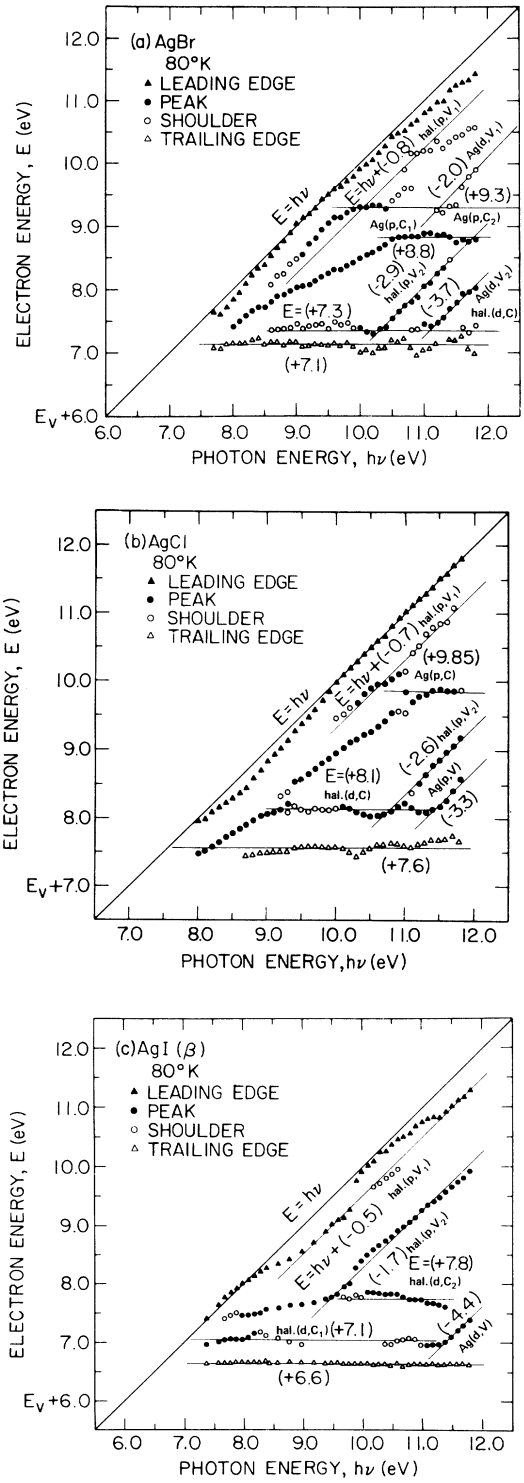

FIG. 3. Spectral distributions of the (a) AgBr, (b) AgCl, and (c) AgI EDC's structure and edges at 80 °K. Unit and zero slope lines, with their electron energy-axis intercepts, are shown fit to appropriate data.

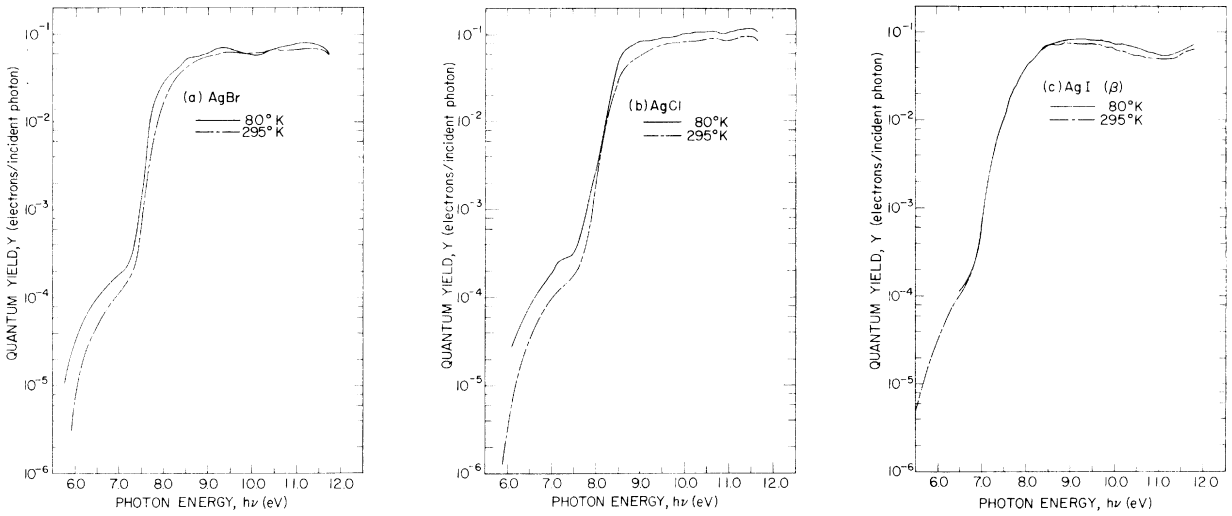

FIG. 4. Comparison of the spectral distributions of the yield of electrons photoemitted per incident photon from (a) AgBr, (b) AgCl, and (c) AgI at 80 and 295 °K.

olating the straight-line portion of the EDC edge just before its maximum slope point. The experimentally broadened high-energy tail is at most 0.2 eV longer than the intercept of the extrapolation with the baseline. The absolute energy scale is then set by fitting a unity-slope line of zero initial-state energy (i.e., $E = h\nu$) to the highest extrapolated points. The resulting scale is independent of temperature since the energy determined by this method for pure valence-state unbroadened structure is independent of temperature, as expected.

The locus of extrapolated trailing-edge points corresponds to the vacuum level. It is a more exact measure of this quantity than the photoemission yield threshold. As seen in Fig. 4, the finite threshold slope causes problems in defining a vacuum level from yield data analogous to those encountered in determining the band gap from optical absorption data. The very small low-photon-energy yield tail below threshold is a measure of the number of electrons which are photoexcited in the metal substrate and then escape through the silver-halide thin-film sample.

The temperature dependence in the structure plots of Fig. 3 does not provide sufficient information to analyze the nature of electronic states. A different data characteristic must be studied since dynamic wave-function hybridization broadens levels without significant shifting. Peak magnitude variations are only quantitatively meaningful when expressed in terms of electrons photoemitted per *absorbed* photon. The required temperature-dependent reflectance is usually not available. Relative magnitude signatures such as peak-to-peak or peak-to-valley ratios are subject to extraneous influences since different final states as well as initial states are involved for any two points on the same EDC. Thus, it is reasonable to focus our attention on the temperature dependence of the EDC width at a fixed fraction of the peak height. This allows identification of hybridized and pure symmetry states as discussed in the introduction. These temperature-dependent characteristics are discussed along with photon-energy variations to give a more complete description of the states involved in the photoemission process.

III. VALENCE STATES

A. Halogen *p* derived

The upper part of the valence band is characterized by two primary regions of large-state density with cause similar photoemission manifestations for all three silver halides. These two features are distinguished from deeper ones by the highly temperature-dependent structure they cause in the EDC's. This is illustrated for AgBr and AgCl in Fig. 1 where the peaks in question are labeled halogen (hal.) p valence [denoted hal.(p, V)].

The photon energy dependence of these structures allows us to identify them as valence-band derived. Averaging the energies determined at room temperature with the 80 °K values in Fig. 3, hal.(p,V_1) density of states is found at −0.8, −0.85, and −0.45 eV relative to the valence-band maximum of AgBr, AgCl, and β-AgI, respectively. Besides the obvious similarity in position dependence on $h\nu$, these structures have a striking magnitude variation with $h\nu$. Examining the series of EDC's in Fig. 5, the upper peak "pops in" at the leading

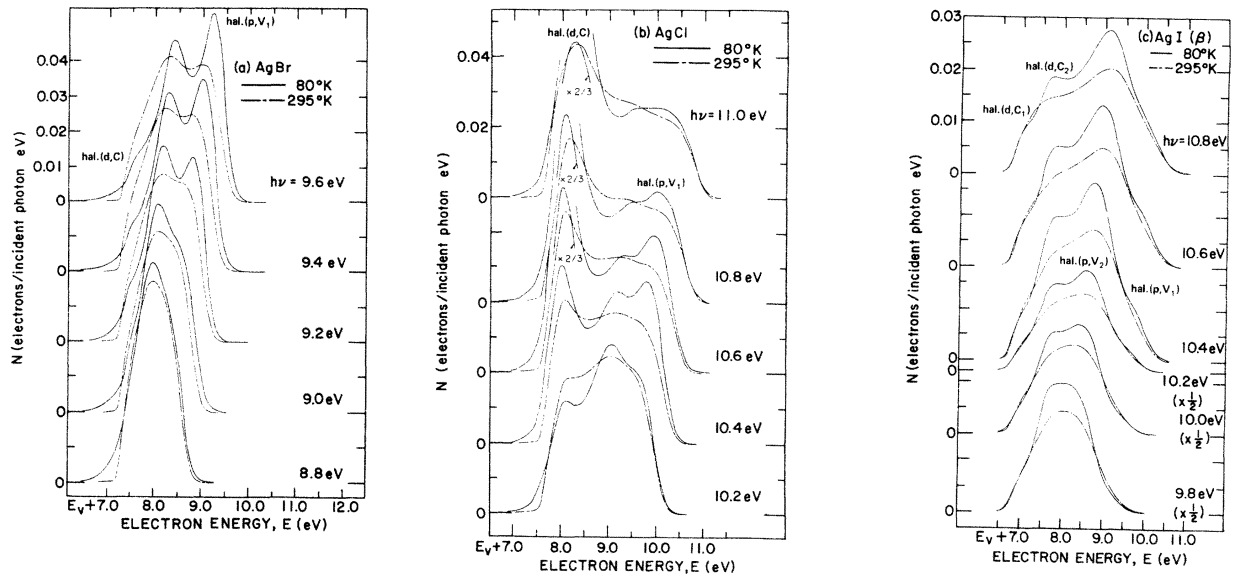

FIG. 5. Comparison of energy distributions normalized to quantum yield (per incident photon) for electrons photoemitted from (a) AgBr, (b) AgCl, and (c) AgI at 80 and 295 °K for the photon energies indicated.

edge of the curves for $h\nu = 9.1$, 10.3, and 10.1 eV, respectively. The abruptness of this appearance (over a 0.1-eV range) at an energy well above threshold must be caused by a strong k-conserving selection rule. Since there subsidiary valence-band maxima along Δ and Σ below the top of the band,[11,12] we presume these structures originate from a high-density-of-states region and go to a conduction band which is changing energy rapidly with k. This is confirmed by the fact that the initial (valence-band) energy of the structure is almost independent of $h\nu$, whereas the final conduction-band energy varies strongly.

The situation is different for β-AgI than for the other silver halides. Note that in AgI [Fig. 5(c)], the most abrupt EDC peak appearance occurs for a deeper valence peak, hal.(p, V_2). The difference in strength of the AgI temperature dependence can be attributed to its lower ionicity.[1] However, the magnitude of the highest valence structure hal.(p,V_1) in AgI is still strongly modulated with $h\nu$ variation, consistent with the other halides; note the high energy shoulder modulation labeled hal.(p,V_1) in Fig. 5(c) and the trend in Fig. 3(c). We thus ascribe this region to non-Γ region state density by analogy to the more studied AgCl and AgBr.

The large difference in behavior of the β-AgI EDC leading edge is quite significant. Note in Fig. 3 that in contrast to AgBr and AgCl, the edge pops abruptly for $h\nu = 9.9$ eV between the valence-band region hal.(p, V_1) and the actual highest valence state defined by the highest points moving as $E = h\nu$. All known cases of a leading edge extrapolation not moving in increments of $h\nu$ are caused by a direct transition from a valence band maximum at Γ.[13] It is the crystal structure of β-AgI which causes this unique feature. While the symmetry of the rock-salt structure for AgBr and AgCl forbids the halogen p states from mixing with Ag 4d orbitals at the center of the zone, the wurtzite symmetry does not force the electronic states to form an indirect band edge in β-AgI. Thus, it is reasonable for us to conclude from the photoemission data that β-AgI has a valence-band maximum at Γ and that it is unique in this regard.

The photon energy dependence of the position of the deeper hal.(p, V_2) structure distinguishes it as originating in the valence band also. From Fig. 3 we see that such regions of high density of states occur at -2.9, -2.65, and -1.7 eV in AgBr, AgCl, and β-AgI, respectively. They are common not only in $h\nu$ position variation, but also in their appearance out of a dominant conduction state structure [labeled by hal.(d, C) in Fig. 3]. As noted with reference to the data of Fig. 5(c), there is evidence that optical transitions from this valence-band region conserve k in β-AgI.

The temperature dependence of all this EDC structure allows us to identify their atomic origin. When the leading peak hal.(p,V_1) emerges in Figs. 5(a) and 5(b), there is a much greater strength at low temperatures. Note how its height in AgBr and AgCl becomes larger than the neighboring peak's as the temperature is lowered. This reversal in the ordering of the relative peak heights

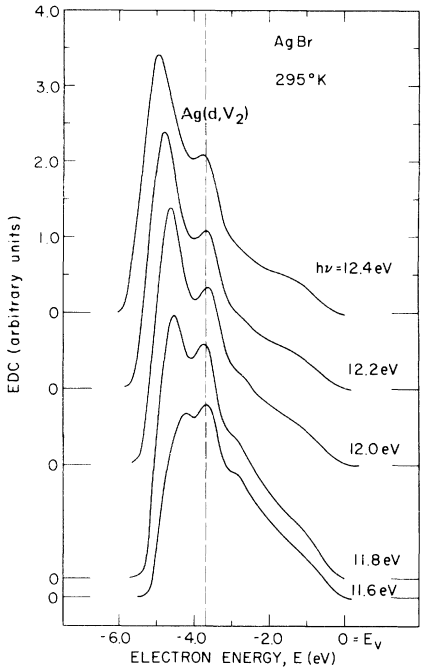

FIG. 6. Comparison of unnormalized energy distributions for electrons photoemitted from AgBr at 295 °K for photon energies of 11.6–12.4 eV. A line is shown at an electron energy of −3.7 eV.

occurs gradually with T as seen in Fig. 1(b). The peak widths are reduced by many times $k_B \Delta T$, and their peak-to-valley ratios are greatly increased. This is true for both hal.(p,V_1) and hal.(p, V_2) as seen in Fig. 1. The strong temperature dependence of hal.(p,V_2) is not limited to just the threshold region but persists for all photon energies where it can be uniquely identified, as seen in Fig. 2(b) for AgCl and Fig. 5(c) for β-AgI (also Fig. 10 below for AgBr).

It is important to note that as shown in Fig. 5 the peak-to-peak spacings and their absolute positions are unaffected by the temperature variation. This is consistent with our interpretations in terms of electronic-state characteristics rather than effects on the photoemission probe being used (e.g., electron transport effects). These very strong temperature variations are due to dynamic modulation of the orbital hybridization. Since the highest filled states in the silver halides are derived from halogen p states,[1,11,12] which mix strongly with lower Ag 4d orbitals, it is reasonable to assign the two structures to halogen p valence electrons [denoted hal.(p, V) above].

It is obvious that the quantum yield cannot be used alone to gain a detailed understanding of the electronic states. Since the yield is a measure of the area under the EDC, the total changes in all the pieces of structure are measured together. Thus, the large structure changes in an EDC such as those for AgBr in Fig. 1(a) result in only a small yield decrease in Fig. 4(a). The effect of cooling on the electron transport in the silver halides is seen in the yield. As shown in Fig. 4 the low-photon energy tail is due to electrons excited in the silver substrate is considerably increased upon cooling. This is probably due to an increased hot electron scattering length in the silver halides at 80°K caused by reduced thermal vibration of the lattice at the low temperature (i.e., freezing out of the optical phonons).[14]

B. Silver 4d derived

The center of the valence band is dominated by a single large density-of-states region. In the photoemission, electrons originating from these states produce structures with a distinctive lack of temperature dependence. Figure 2 shows this behavior quite well for AgBr and AgCl by the peaks labeled silver d valence [Ag(d, V_2) and Ag(d, V) respectively]. (Figure 10 presents AgBr results for a number of photon energies.) The photon energy dependence of such EDC structures (summarized in Fig. 3) identifies these as originating from filled states −3.7, −3.3, and −4.4 eV below the valence-band maximum. While this feature is just emerging above threshold near the normal 11.8-eV experimental cutoff, it shows the same characteristics at much higher energies. As seen in Fig. 6, a strong AgBr peak originating at −3.7 eV continues in room-temperature "windowless"

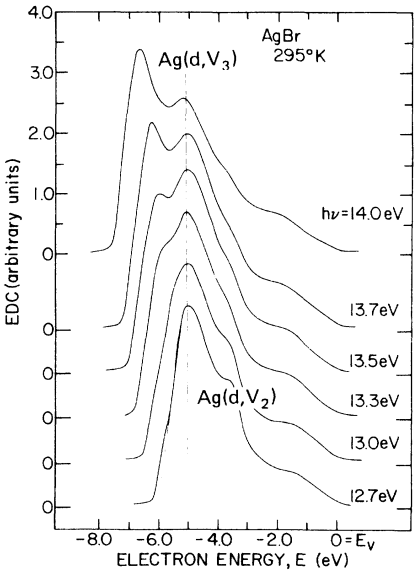

FIG. 7. Comparison of unnormalized energy distributions for electrons photoemitted from AgBr at 295 °K for photon energies of 12.7–14.0 eV. A line is shown at an electron energy of −5.0 eV.

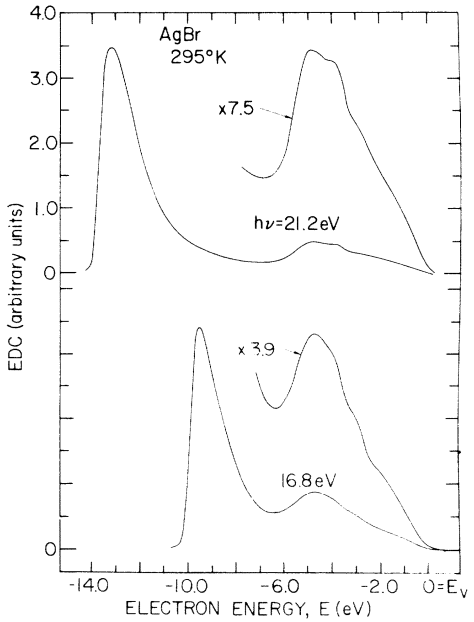

FIG. 8. Comparison of unnormalized energy distributions for electrons photoemitted from AgBr at 295 °K for photon energies of 16.8 and 21.2 eV. Part of each curve is expanded by the factor shown.

data.

We observe that these states lie very close in energy to the hybridized halogen p valence electrons hal.(p, V_2) in all these materials (within 1 eV in AgBr and AgCl). Thus the criteria governing dynamic hybridization effects are met for these levels. The characteristic temperature independence of these states must be a property of unhybridized atomic orbitals, which most likely have orbital quantum number greater than that of p electrons.[1] The pure component of Ag $4d_{5/2}$ electrons is thereby accurately located.

The remaining Ag $4d_{5/2}$ electrons have orbitals which hybridize with the higher-lying halogen p orbitals. In AgBr, we are able to identify a density-of-states region associated with these hybridized Ag d electrons lying above the pure d states. Note in Fig. 3(a) that for photon energies $h\nu \geq 11.2$ eV, the 80 °K EDC's exhibit a shoulder which originates from valence states −2.0 eV below the band maximum. This is an easily identifiable feature as seen in the data of Fig. 2(a) labeled Ag(d, V_1) (note, the sample used for Fig. 10 exhibits this structure more distinctly). We can use the fact that this peak does not appear until 11.2 eV to identify it as Ag $4d$ in origin. As summarized in Fig. 3(a), the strength and nature of EDC structure varies considerably when final states greater than 9.3 eV are reached. We will show in Sec. III that this is due to the change in atomic character of the conduction states from halogen d to Ag $5p$. The preferential increase in oscillator strength associated with exciting predominantly Ag $4d$-derived electrons to p rather than d final states makes this rather small filled density of states feature observable in the photoemission. Its absence in the other silver halide data is likely due to the Ag $5p$ conduction states lying higher in energy (> 10 eV in AgCl and AgI) rather than an accidental near degeneracy with the unhybridized Ag $4d_{5/2}$ states [e.g., compare Fig. 12(a) and (b) at X]. In Sec. V, we will identify these structures in AgCl and AgI by comparison with x-ray photoemission, where the oscillator strength for d-state excitations is large.

The remaining Ag $4d$ electrons originate from $4d_{3/2}$ orbitals and from a band deeper in the valence states. This region was investigated by windowless measurements for AgBr at room temperature. As seen in Fig. 7, the EDC's above 12.7 eV are characterized by a strong peak originating −5.0 below the valence-band maximum. Having identified the halogen p states and Ag $4d_{5/2}$ levels, it is reasonable to assign these transitrons to a high-state density derived from Ag $4d_{3/2}$ orbitals. These states are probably hybridized strongly with the higher-energy halogen p states. Then dynamic thermal changes in halogen electron energies of $> 10\, k_B \Delta T$ will be nearly balanced by opposite changes in these Ag-derived levels since the net energy change can only be $k_B \Delta T$. Temperature-dependent photoemission of these states would be a valuable test of this identification. Note that the $4d_{3/2}$ origin of such states is consistent with the large measured temperature dependence of the Γ_{12} conduction level in KBr (see discussion in Sec. V B. of Ref. 1).

C. Band width

At very high photon energies an overview of the entire valence band is obtained. Because of the altered selection rules for transitions to such high final states, the AgBr EDC's shown in Fig. 8 are rather featureless, reflecting mainly the two primary Ag $4d$ bands at −3.7 and −5.0 eV. Ignoring the large electron-electron scattering peak at the left end of the curves (i.e., threshold), the area under these d peaks is more than half the total area under this part of the EDC. This is consistent with the 5:3 ratio of d-to-p states comprising the valence band. The trailing edge extrapolation of this portion of the high-energy EDC's directly yields the valence-band width. As seen in Fig. 8, valence-band transitions rise out of the background beginning about −6 eV below the top of the filled states.

IV. CONDUCTION STATES

The 5s states derived from the Ag^+ ion form the conduction-band minimum at Γ. Unfortunately, they are below the vacuum level and therefore inaccessible to photoemission. Attempts to reduce the vacuum level sufficiently to yield a negative electron affinity were unsuccessful since Cs reacted with the silver halides. However, we are able to definitively identify higher conduction state features. Assignments are most straightforward in AgCl where only one Cl 3d and one Ag 5p high-density-of-states region were observed. Additional Ag 5p structure in AgBr and I 5d structure in β-AgI can be identified by analogy to the characteristic trends in the simpler AgCl data.

A. Halogen d derived

In the electron energy range just above threshold, there is a large conduction band density of states peak in all the silver halides. As seen in Fig. 5(b), this dominates the AgCl spectra as the strong structure fixed at $E = 8.1$ eV. This structure has very distinguishable characteristics with photon energy variation. As summarized in Fig. 3(b), two strong valence-band structures [hal.(p,V_2) and Ag(d, V)] emerge from this peak. If we then study the AgBr structure plot Fig. 3(a), it is clear that the corresponding valence peaks in this material are also emerging from a region of high conduction-state density at $E = 7.3$ eV. Since this is only 0.2 eV above the vacuum level, it appears only as a shoulder near the EDC trailing edge [Figs. 5(a) and 11].

The situation is a bit different for AgI as seen in Fig. 3(c). The lower I 5p valence peak emerges from a conduction state region at $E = 7.8$ eV which is different from the 7.1-eV origin of the Ag 4d peak. However, both these EDC peaks [hal.(p, V_2) and Ag(d, V)] behave the same with $h\nu$ variation as their counterparts in the other halides. Thus, we identify both conduction-band peaks as being derived from I 5d states.

The 0.7-eV splitting is quite prominent in the AgI data. At low-photon energies shown in Fig. 9, the shift in strength between the two peaks at 80°K is dramatic. This distinction is present at higher $h\nu$ as well [see Fig. 5(c)]. Equally important is the complete smearing of this halogen d conduction hal.(d, C) separation at room temperature; note that only one EDC peak is present at 295 K for $h\nu = 8.0$ and 8.2 eV in Fig. 9. The broadening of both these peaks obeys the same relation[1]: $W = 0.29 \exp(1.3 \times 10^{-3}\, T/\Theta_D)$. This points to the same atomic origin for both conduction state densities. Further, there is a very strong dynamic hybridization of these I 5d states

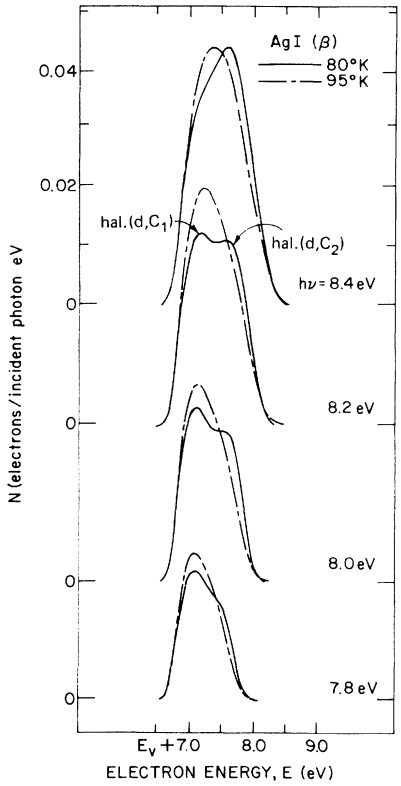

FIG. 9. Comparison of energy distributions normalized to quantum yield (per incident photon) for electrons photoemitted from AgI at 80 and 295 °K for the photon energies indicated.

with the higher-lying Ag 5p empty levels. An equivalent broadening for the Ag 5p states is discussed below for AgBr. The low-temperature 0.7-eV splitting of the d states is probably a measure of the X-L conduction band separation in β-AgI. The X point is most likely lower, as discussed in Sec. V.

B. Silver 5p derived

Returning our attention to AgCl, a conduction-band density-of-states peak is easily identified at $E = 9.85$ eV from Fig. 3(b). Simply from the ordering of the silver and halogen states one would identify this structure as Ag 5p derived. Independent evidence for this interpretation comes from recognizing that the nature of transitions from filled p states changes for photon energies which excite electrons to these final states. In Fig. 5(b), it is clear that the hal.(p, V_1) structure is strongly attenuated as $h\nu$ is increased from 10.6 to 11.0 eV, and is only a slight shoulder above 11.0 eV [see Fig. 2(b)]. In Fig. 3(b) we note that this reduction from peak to shoulder status continues for all $h\nu > 10.6$ eV. This would be con-

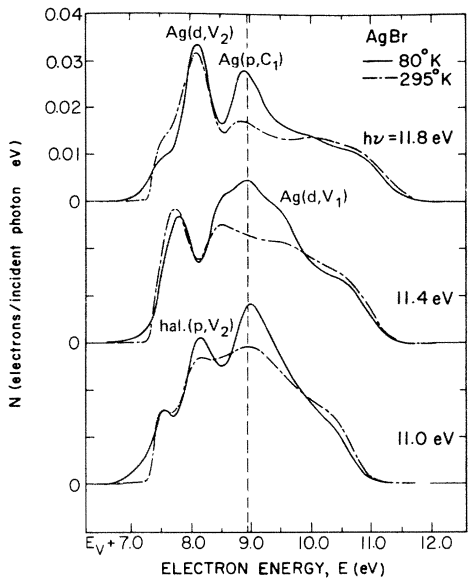

FIG. 10. Comparison of energy distributions normalized to quantum yield (per incident photon) for electrons photoemitted from AgBr at 80 and 295 °K for the photon energies indicated. A line is shown at an electron energy of about 8.8 eV.

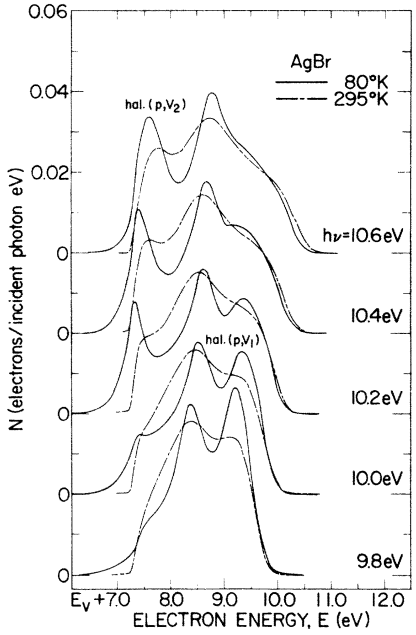

FIG. 11. Comparison of energy distributions normalized to quantum yield (per incident photon) for electrons photoemitted from AgBr at 80 and 295 °K for photon energies of 9.8–10.6 eV.

sistent with the conduction states changing from mixed d-p status to predominantly p character, thereby leading to mainly p-p transitions which are dipole forbidden.

This silver p-conduction [Ag(p,C)] structure has two distinguishing EDC effects as summarized in Fig. 3(b). A "jog" in the locus of the hal.(p,V_1) peak positions occurs as it passes through the conduction-band peak (at $h\nu \simeq 10.5$ eV). Further, the peak itself causes a strong structure for $T = 80$ °K in the EDC at the final-state position as seen also in Fig. 2(b). These two features are seen separately in AgBr [see Fig. 3(a)], suggestive of two conduction-band peaks having a Ag 5p origin. The EDC peak at $E = 8.8$ eV is very prominent as shown in Fig. 10. It dominates the EDC's at these high-photon energies. The hal.(p,V_1) "jog" is definitively seen at $E = 9.3$ eV as shown in Fig. 3(a). This also leads to some flattening of the Ag(d, V_1) structure as it passes through these final states. The change in the character of EDC structure for higher $h\nu$ is as dramatic as we observed for AgCl. In Fig. 11, the highest EDC structure is completely washed out as $h\nu$ is increased from 9.8 eV through 10.6 eV. In Fig. 7, we also observe that the final states change character around $E = 9.3$ eV, since the −3.7-eV valence structure [i.e., Ag(d, V_2)] is attenuated beginning with $h\nu = 13.0$ eV. The 0.5-eV splitting of the two Ag 5p-derived conduction density-of-states peaks in AgBr is probably characteristic of the L-X dispersion in this band.

If the halogen d-derived conduction structure exhibits strong thermal broadening of the orbital hybridization, then the Ag 5p states with which they hybridize must exhibit comparable broadening. In AgCl this is somewhat evident from the washing away of the Ag(p, C) peak at $h\nu = 11.6$ eV in Fig. 2(b) as the temperature is raised. It is particularly clear for AgBr. In Fig. 10, the Ag(p, C_1) peak at $h\nu = 11.4$ eV is completely broadened out at room temperature. Note in Fig. 2(a) that this disappearance is gradual with temperature, indicating a process tied to the ionic vibrational amplitude rather than any order-disorder transformation. The Ag(p, C_2) peak is very difficult to identify from the room-temperature structure plots. The broadening for both peaks caused by raising the temperature through the Debye value is estimated to be between 0.5 and 1.0 eV.

In β-AgI the Ag 5p states cannot be seen as a high-density-of-states region. This probably indicates that these p states lie greater than 11.5 eV above the valence-band minimum. From the assignment of the AgI valence-band maximum to Γ states, we can identify the final-state regions of high Γ-state density by using the strong leading edge modulation caused by the k-conservation selection rule. Since from Fig. 3(c) the highest valence states only cause transitions to conduction states at 8.0 and 10.1 eV (±0.2 eV), we ex-

pect these to be the locations of Γ states. The former is probably I $5d$ derived (i.e., $\Gamma_{2'}$) because of its proximity in energy to hal.(d, C_2), while the 10.1-eV states are likely Ag $5p$ in origin (i.e., Γ'_{25}) by analogy to the other halides.

V. DISCUSSION

A. Experiment

The density-of-states structure identified in this study is summarized in Table I along with the assignments discussed above. The results of other photoelectron-spectroscopy experiments are included for comparison. The other data concern exclusively valence-state properties. There is good agreement on the position of the Ag $4d_{5/2}$ states for all three silver halides among all measurements except Mason's.[4] There appears to be a ~0.4 eV underestimate of the d energies in his measurements possibly due to inaccurate determination of the bulk Fermi level of the silver halides. Perhaps exposure to the ambient in that work caused a surface band bending of this magnitude. Most of his other results are brought into agreement by adding this energy to all the values, as we have done in Table I.

Note that the highest x-ray photoemission (XPS) peaks then do not agree with our halogen valence

TABLE I. Summary of high electron-state-density regions in the silver halides. The energies are accurate to ±0.1 eV for AgBr and AgCl, and ±0.2 eV for β-AgI (except as noted). Symbols used to identify structure in the EDCs [e.g., the second conduction-band structure having Ag p character–Ag(p, C_2)] are included for reference.

Material	Energy (eV)	Assignment	Other experiments
AgBr	9.3	Ag$(5p)$–Ag(p, C_2)	
	8.8	Ag$(5p)$–Ag(p, C_1)	
	7.3	Br$(4d)$–hal.(d, C)	
	7.15	vacuum level	
	0	valence-band maximum	
	−0.85	Br$(4p)$, Δ or Σ–hal.(p, V_1)	
	−1.95	Ag$(4d)$–Ag(d, V_1)	−2.0 ±0.4[a]
	−2.9	Br$(4p)$, L–hal.(p, V_2)	−2.86 ±0.1[a]
	−3.3	bottom of Br$(4p)$ band	
	−3.7	Ag$(4d_{5/2})$–Ag(d, V_2)[b]	−3.8,[c] −3.57 ±0.1,[a] −3.8[d]
	−5.0	Ag$(4d_{3/2})$–Ag(d, V_3)	−4.6 ±0.1[a]
	−6.0	bottom of valence band	−5.9[c]
AgCl	9.85	Ag$(5p)$–Ag(p, C)	
	8.1	Cl$(3d)$–hal.(d, C)	
	7.55	vacuum level	
	0	valence-band maximum	
	−0.8	Cl$(3p)$, Δ or Σ–hal.(p, V_1)	
	(−1.6)	Ag$(4d)$	−1.6 ±0.4[a]
	−2.65	Cl$(3p)$, L–hal.(p, V_2)	−2.7 ±0.2[a]
	−3.0	bottom of Cl$(3p)$ band	
	−3.3	Ag$(4d_{5/2})$–Ag(d, V)[b]	−3.5,[c] −3.4±0.1,[a] −3.4[d]
AgI(β)	10.1	Ag$(5p)$, $\Gamma_{2'}$	
	8.0	I$(5d)$, $\Gamma_{25'}$	
	7.8	I$(5d)$, L–hal.(d, C_2)	
	7.1	I$(5d)$, X–hal.(d, C_1)	
	6.6	vacuum level	
	0	valence-band maximum, Γ	
	−0.45	I$(5p)$, Δ or Σ–hal.(p, V_1)	
	(−1.1)	Ag$(4d)$	−1.06 ±0.2[a]
	−1.7	I$(5p)$, L–hal.(p, V_2)	−1.35[e]
	−4.4 ±0.1	Ag$(4d_{5/2})$–Ag(d, V)[b]	−4.15,[f,e] −4.3,[c] −4.47 ±0.1[a]

[a] Reference 4 (values adjusted by −0.4 eV).
[b] Negligible mixing with states of other atomic origin.
[c] Reference 3 (±0.2 eV).
[d] Reference 2 (±0.1 eV).
[e] Reference 6 (±0.15 eV).
[f] Reference 5 (±0.1 eV).

assignment [hal.(p,V_1)]. Using the adjusted values, the first XPS peak agrees with our Ag 4*d* assignment [Ag(d, V_1)] in AgBr. Further, we expect the XPS measurements to be more sensitive to the *d*-component states.[2] This all suggests that the highest-energy XPS components in all the halides are Ag 4*d* derived rather than Mason's halogen identification. These values are included for the other halides in parentheses in Table I. Like the higher, mainly *p* band [hal.(p,V_1)] originating from the Γ_{15} below, this 4*d* density of states originates from the same Γ_{15} state, which is now at *higher* energies. Ours are the first measurements of the halogen *p* density-of-states peak, which falls within the zone along Δ or Σ [i.e., hal.(p, V_1)].

The remaining valence-band interpretations are consistent with the other photoemission and optical results. Of particular note is the unique assignment of the valence-band maximum in β-AgI to the Γ point based on the EDC leading edge behavior. Cardona[15] used the strength of the exciton absorption spectrum to predict the occurrence of direct allowed transitions originating from I *p*-derived states at the center of the zone.

This work reports the first conduction-band features identified by photoemission. Comparison can only be made with optical property interpretations. The far-uv-studies of Carrera and Brown[16] on AgCl are particularly valuable in this regard. Recall that we used AgCl in Sec. IV as a basis for identifying conduction-state features common to all three silver halides. There were only two high-density-of-states regions at $E = 8.1$ and 9.85 eV. From the ordering of the bands and the peak temperature dependence we identified the former as Cl 3*d* derived and the latter as Ag 5*p* in origin. By comparison to KCl, Carrera and Brown[16] located the Cl-3*d*, $\Gamma_{25'}$ state at 8.3 eV and the Ag-5*p*, $\Gamma_{2'}$ state at 9.9 eV. This excellent agreement is valuable support for all our conduction-band assignments.

The values of the pure silver-halide vacuum levels are included in Table I since electron affinities are vital to theories of photographic sensitivity.[17]

B. Band structure

We find that the speculative AgBr and AgCl band structure of Bassani, Knox, and Fowler[11] gives a surprisingly good general description of not only the valance states but also the conduction bands. The augmented-plane-wave calculations of Scop[12] do not yield reasonable agreement contrary to findings based on optical properties alone.[18] Our experimentally determined regions of high density of states are superimposed on these bands in Fig. 12. A similar diagram for β-AgI could be constructed using the numbers in Table I. The most striking agreement is the coincidence of the Ag states with almost pure 4*d* symmetry at −3.7 and −3.3 eV in AgBr and AgCl respectively. These flat bands (and by implication the AgI states at −4.4 eV) are composed of localized states which are not significantly hybridized.[19] This is in agreement with our dynamic hybridization model which correctly identified such states by their temperature independence.

The other valence structure suggests corrections to the theoretical band structures of the order of 0.5 eV. For examples, the AgBr valence-

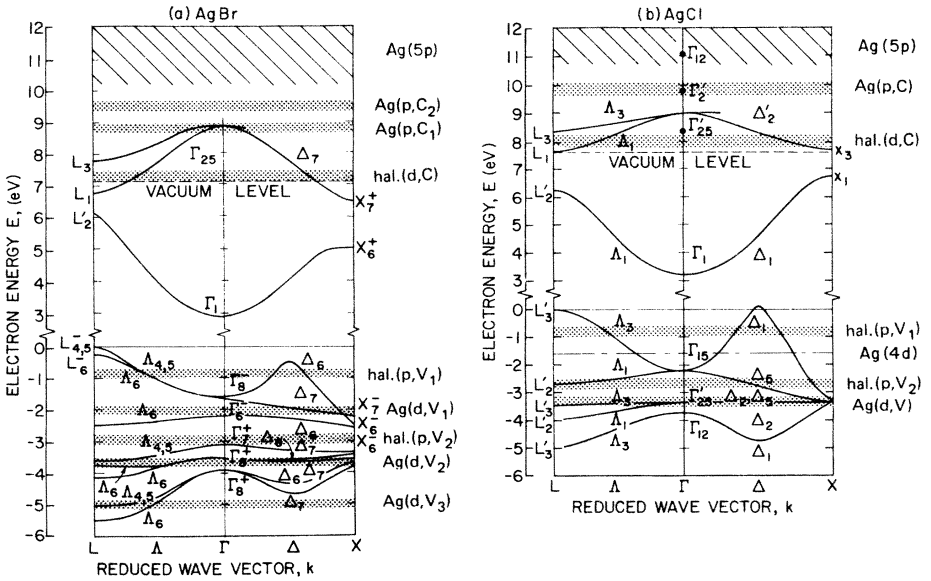

FIG. 12. Electronic band structure of (a) AgBr and (b) AgCl as speculated by Bassani, Knox, and Fowler (Ref. 11) with the estimates for the Ag(5*p*) states (slashed area) by Seitz (Ref. 20) and the AgCl conduction states at Γ by Carrera and Brown (Ref. 16). The atomic designations are the orbitals from which the states at Γ are derived. The vacuum level (---) and regions of high density of states (shaded) determined from these studies are superimposed on these bands. The Ag(4*a*) states in AgCl (——) are deduced using the XPS data of Ref. 4.

band widths are too narrow, the Δ (or Σ) relative maximum too high, and Γ_{15} location displaced by this amount from experiment. The second halogen valence peak [hal.(p, V_2)] occurs at L in AgCl but is high by 0.5 eV in AgCl. Using this L_2' assignment for this structure, the conduction-band splitting of I $5d$-derived states in β-AgI is estimated to be 0.7 eV from placement of hal.(d, C_1) at X and hal.(d, C_2) at L. Similarly, by deducing that the AgI valence-band maximum is at Γ, we used k-conservation selection rules to identify the I $(5d)$ $\Gamma_{25'}$ conduction state at 8.0 ± 0.2 eV and the Ag $(5p)$ $\Gamma_{2'}$ state at 10.1 ± 0.2 eV. This general location of the Ag $5p$ conduction states is further in agreement with the estimate of Seitz[20] for the separation of Ag $5p$ and $5s$ states in the silver halides.

These comparisons serve to substantiate the electronic structure results determined by our studies. Since these assignments were made on the basis of the temperature dependence of the EDC's as interpreted using the dynamic hybridization model, this agreement is further evidence for such a description of photoemission for partially ionic solids.[1] The valence-band assignments are the most complete to date, supporting recent attempts[2,21] at silver-halide band calculations. A description of the conduction band is now available for the first time. This should stimulate detailed calculations of these states.

ACKNOWLEDGMENTS

This work benefited from expert technical assistance of the Stanford Tube Laboratory. We gratefully acknowledge stimulating discussions with Professor F. C. Brown, Professor W. B. Fowler, and Professor J. J. White III.

*All experimental work was done at Stanford University under NASA Contract No. NGR 05-020-066.
[1]R. S. Bauer, S. F. Lin, and W. E. Spicer, preceding paper, Phys. Rev. B 14, 4527 (1976).
[2]J. Tejeda, N. J. Shevchik, W. Braun, A. Goldmann, and M. Cardona, Phys. Rev. B 12, 1557 (1975).
[3]D. R. Williams, J. G. Jenkin, R. C. G. Leckey, and J. Liesegang, Phys. Lett. A 49, 141 (1974).
[4]M. G. Mason, Phys. Rev. B 11, 5094 (1975).
[5]D. E. Eastman, W. D. Grobman, J. L. Freeouf, and M. Erbudak, Phys. Rev. B 9, 3473 (1974).
[6]A. Goldmann, J. Tejeda, N. J. Shevchik, and M. Cardona, Phys. Rev. B 10, 4388 (1974).
[7]R. S. Bauer, Ph.D. dissertation (Stanford University, 1970) (unpublished) (Xerox University Microfilms No. 71-19646).
[8]S. F. Lin, W. E. Spicer, and R. S. Bauer, following paper, Phys. Rev. B 14, 4551 (1976).
[9]T. H. DiStefano and D. T. Pierce, Rev. Sci. Instrum. 41, 180 (1970).
[10]R. C. Eden, Rev. Sci. Instrum. 41, 252 (1970).
[11]F. Bassani, R. S. Knox, and W. B. Fowler, Phys. Rev. 137, A1217 (1965).
[12]P. M. Scop, Phys. Rev. 139, A934 (1965).
[13]See for example, W. E. Spicer and R. C. Eden, in *Ninth International Conference on the Physics of Semiconductors, Moscow, July 23–29, 1968* (Nauka, Leningrad, 1968), Vol. 1, p. 65; W. E. Spicer, in *Optical Properties of Solids—New Developments*, edited by B. O. Seraphin (North-Holland, Amsterdam, 1976).
[14]T. H. DiStefano and W. E. Spicer, Phys. Rev. B 7, 1554 (1973).
[15]M. Cardona, Phys. Rev. 129, 69 (1963).
[16]N. J. Carrera and F. C. Brown, Phys. Rev. B 4, 3651 (1971).
[17]See, for example, H. Meier, *Spectral Sensitization* (Focal, New York, 1968).
[18]J. J. White III, J. Opt. Soc. Am. 62, 212 (1972); R. S. Bauer, W. E. Spicer, and J. J. White III, *ibid.* 64, 830 (1974).
[19]P. M. Scop, MIT Solid State and Molecular Theory Group, Quarterly Progress Report No. 54, 1964 (unpublished), p. 15.
[20]F. Seitz, Rev. Mod. Phys. 23, 328 (1951).
[21]W. B. Fowler, Phys. Status Solidi B 52, 591 (1972).

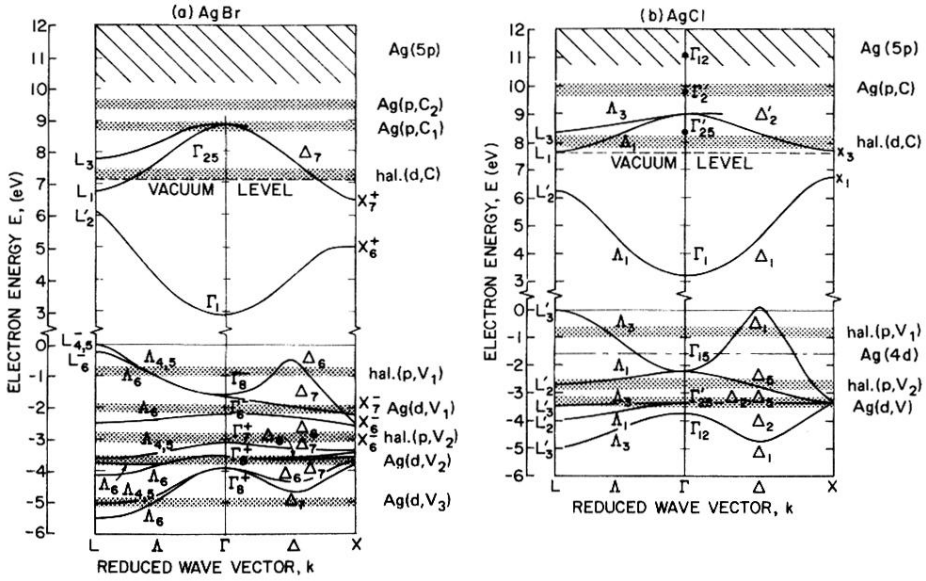

FIG. 12. Electronic band structure of (a) AgBr and (b) AgCl as speculated by Bassani, Knox, and Fowler (Ref. 11) with the estimates for the Ag(5*p*) states (slashed area) by Seitz (Ref. 20) and the AgCl conduction states at Γ by Carrera and Brown (Ref. 16). The atomic designations are the orbitals from which the states at Γ are derived. The vacuum level (---) and regions of high density of states (shaded) determined from these studies are superimposed on these bands. The Ag(4*d*) states in AgCl (——) are deduced using the XPS data of Ref. 4.